

# Highlights

## Numerical methods for localization

Rudolf A. Römer

- the article reviews existing numerical algorithms used when studying Anderson localization and gives relevant references
- algorithms for data generation
  1. diagonalization strategies such as exact methods, sparse-matrix methods, kernel-polynomial methods
  2. iterative/quasi-1D algorithms such as the transfer-matrix and the Green function method
  3. renormalization-inspired numerical approaches
- data analysis algorithms
  1. energy-level and -ratio statistics
  2. wave function statistics and multi-fractal analysis
  3. finite-size scaling algorithms, with and without assuming a scaling form
- current challenges
  1. numerical algorithms in use for data generation and analysis of interacting disordered systems
  2. algorithms based on machine learning strategies

# Numerical methods for localization

Rudolf A. Römer

*<sup>a</sup>Department of Physics, University of Warwick, Gibbet Hill Road, Coventry, CV4 7AL, West Midlands, United Kingdom*

---

## Abstract

Anderson localization provides a challenge to numerical approaches due to the inherent randomness, and hence absence of simple symmetries, in its discrete Hamiltonian representation. Numerous algorithmic approaches have been developed or adopted from other fields and have been collected in this encyclopedia entry. In the discussions below, the emphasis is on the numerical algorithms for localization, while the discussion of the physics of localization is referred to in companion entries by Elgart and Oganessian in this encyclopedia.

*Keywords:* exact diagonalization, sparse matrix diagonalization, recursive diagonalization methods, transfer-matrix method, Green function method, numerical renormalization group methods, decimation method, energy-level statistics, wave function statistics, energy ratio statistics, multi-fractal analysis, finite-size scaling, density-matrix renormalization group, strong disorder renormalization group, machine learning

---

## 1. Introduction

Anderson localization, as reviewed in this encyclopedia in the entries by Elgart and Oganessian, cannot be solved analytically in dimensions two and above (Stollmann, 2001). Hence much effort has been focused on developing efficient numerical tools. In its usual form, the discrete Anderson Hamiltonian (Anderson, 1958) is given by the matrix elements

$$H_{\mathbf{ab}} = \varepsilon_{\mathbf{a}}\delta_{\mathbf{ab}} - t_{\mathbf{ab}}\delta_{\langle\mathbf{a},\mathbf{b}\rangle}, \quad (1)$$

where  $\varepsilon_{\mathbf{a}}$  is the potential onsite disorder and  $\delta_{\mathbf{ab}}$  the Kronecker delta, while  $t_{\mathbf{ab}}$  denotes the kinetic hopping energy with  $\delta_{\langle\mathbf{a},\mathbf{b}\rangle}$  non-zero when lattice sites  $\mathbf{a} = (a_1, a_2, \dots, a_d)$ ,  $\mathbf{b} = (b_1, \dots, b_d)$  are within a defined distance relationship on a

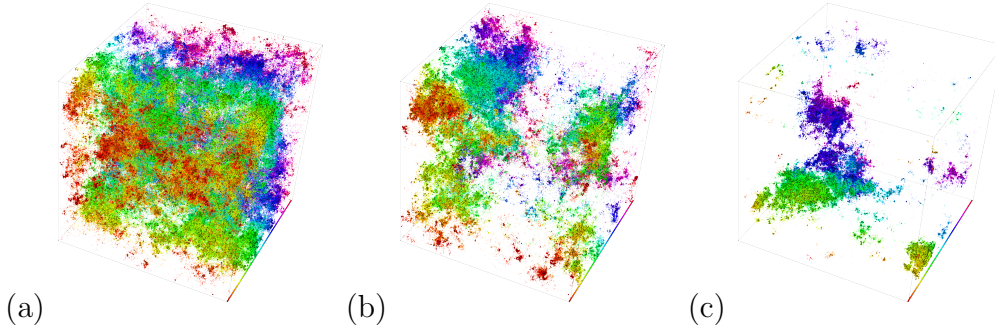


Figure 1: (a) Extended, (b) critical and (c) localized wave function probabilities for the three-dimensional Anderson model with periodic boundary conditions at  $E \approx 0$  with  $N = 200^3$  and  $W = 15, 16.5$  and  $18$ , respectively. Every site  $\mathbf{a}$  with probability  $|\psi_{\mathbf{a}}|^2$  larger than the average  $1/|\mathcal{L}_3|$  is shown as a box with volume  $|\psi_{\mathbf{a}}|^2|\mathcal{L}_3|$ . Boxes with  $|\psi_{\mathbf{a}}|^2|\mathcal{L}_3| > \sqrt{1000}$  are plotted with black edges. The color scale along the bottom right edge distinguishes between different slices of the system. The eigenstates have been computed with JADAMILU (Bollhöfer and Notay, 2007) as described by Schenk et al. (2008).

discrete,  $d$ -dimensional lattice  $\mathcal{L}_d$  — usually the nearest-neighbor separation on  $\mathcal{L}_d$ . With  $|\mathcal{L}_d|$  counting the number of lattice sites,  $H_{\mathbf{ab}}$  is an  $|\mathcal{L}_d| \times |\mathcal{L}_d|$  matrix. The time-independent single-particle Schrödinger equation can then be written as

$$\varepsilon_{\mathbf{a}}\Psi_{\mathbf{a}} - \sum_{\mathbf{b} \in \mathcal{L}} t_{\mathbf{ab}}\delta_{\langle \mathbf{a}, \mathbf{b} \rangle} \Psi_{\mathbf{b}} = E\Psi_{\mathbf{a}} \quad (2)$$

with  $\Psi_{\mathbf{a}} = \Psi_{a_1, \dots, a_d}$  the coefficients of the wave function  $\Psi = \sum_{\mathbf{a} \in \mathcal{L}_d} \Psi_{\mathbf{a}} |\mathbf{a}\rangle$  in a suitable basis  $|\mathbf{a}\rangle$  and  $E$  the energy.

In its simplest form, the Hamiltonian (1) is studied on a  $d$ -cubic lattice with  $t_{\mathbf{ab}} = t_{\mathbf{ba}} = t = 1$  for all nearest-neighbors  $\mathbf{a}, \mathbf{b}$  and  $\varepsilon_{\mathbf{a}}$  independent and identically distributed random numbers  $\in [-W/2, W/2]$ . Hence the parameter  $W/t$  expresses the strength of the disorder. See Fig. 1 for examples of  $\Psi$  in  $d = 3$ . Since numerical studies of Anderson localization began to emerge in the late 1970s, this set-up has of course been much varied to include more complicated situations (Kramer and MacKinnon, 1993). Examples include variations in  $d$  from 1 to  $\infty$ , changes in the lattice structure, symmetry and topology, changes to and additional disorder or correlations in the  $\varepsilon_{\mathbf{a}}$  and  $t_{\mathbf{ab}}$ , as well as inclusion of spin-, external field and interaction effects (Brandes and Kettemann, 2003). The common theme unifying all the studies is the absence of symmetries in  $H$  due to the disorder which in turn prevents a simple restructuring of the matrix into much smaller irreducible blocks (Ev-

ers and Mirlin, 2008). Connecting the properties of such a single large-block matrix with the physics of Anderson localization is the challenge taken on by the numerical algorithms listed in this encyclopedia entry.

## 2. Exact diagonalization

Given an invertible matrix (1), the most straightforward approach is to use standard *full* matrix methods to compute eigenvalues and eigenvectors such as given by the LAPACK library routines (Anderson et al., 1999) and their many highly optimized implementations. At the time of writing this entry, matrices of sizes up to  $\sim 10^4 \times 10^4$  can be readily studied with this method. However, as an average over many different disorder realizations is always necessary to find physically reliable results, already such matrix sizes can lead to many weeks of computing. Many of the algorithms mentioned below were conceived to allow for faster availability of results, while at the same time leading to a more limited set of computed information.

When  $\delta_{\langle \mathbf{a}, \mathbf{b} \rangle}$  is sufficiently short-ranged, many of the matrix elements  $H_{\mathbf{ab}}$  are equal to 0. In this case, it can be advantageous to use *sparse* matrix methods. Such methods construct selected regions of the eigenspectra using repeats of an optimized matrix-vector product computation for  $H_{\mathbf{ab}}\Psi_{\mathbf{b}}$  following the classic power series algorithm (Horn and Johnson, 1985). For the Anderson problem, the implementation of the Lanczos variant by Cullum and Willoughby (2002) is particularly useful since the disorder removes spectral degeneracies such that the "ghost eigenvalues" coming from the implementation can be readily identified. Coupling the sparse-matrix approach with advantages in iteratively solving coupled systems of equations, Schenk et al. (2008) found that a Jacobi-Davidson approach can construct eigenstates of size up to  $350^3 \times 350^3$  in the numerically most demanding region around the centre of the spectrum within a reasonable time. Weiße et al. (2006) showed that similar sizes can be reached using kernel-polynomial methods when coupled with efficient recursive polynomial expansion techniques. The method is particularly efficient in determining a change in the *distribution* of the local density of states as a criterion for Anderson localization.

## 3. Quasi 1D methods

Repeated matrix-vector computations also underlie the celebrated transfer-matrix method (TMM) (Pichard and Sarma, 1981, MacKinnon and Kramer,

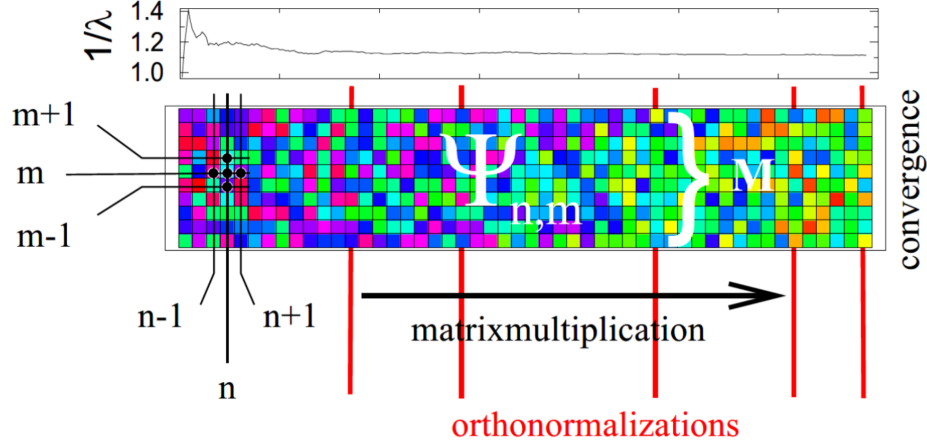


Figure 2: Schematic diagram of the TMM method for the example of a  $d = 2$  Anderson model. At slice  $n$  and position  $m$ , one needs to know the (past)  $\psi_{n-1,m}$  value, the (present) values of  $\psi_{n,m}$  and  $\psi_{n,m\pm 1}$  and then compute the (future) value of  $\psi_{n+1,m}$ . The red lines indicate the orthogonalizations for  $\psi$  needed for numerical stability. The diagram at the top shows the behavior of the typical convergence for a Lyapunov exponent measured after each reorthonormalization, the actual number of reorthonormalization used here exceeds  $10^4$ . The colors of  $\psi_{n,m}$  are chosen such that they indicate the eventual convergence for  $n \rightarrow \infty$ .

1983). The main idea is that it is often possible for a suitable  $\mathcal{L}$  to rewrite (2) as

$$\begin{pmatrix} \psi_{n+1} \\ \psi_n \end{pmatrix} = \begin{pmatrix} \tau_{\langle n+1,n \rangle}^{-1} (E\mathbf{1} - \mathbf{H}_{\mathbf{d}-1}) & -\tau_{\langle n+1,n \rangle}^{-1} \tau_{\langle n,n-1 \rangle} \\ \mathbf{1} & \mathbf{0} \end{pmatrix} \begin{pmatrix} \psi_n \\ \psi_{n-1} \end{pmatrix}. \quad (3)$$

Here,  $\psi_n = (\psi_{n,1}, \dots, \psi_{n,|\mathcal{L}_{d-1}|})$  are transfer states along a single spatial coordinate in  $\mathcal{L}$  while  $\mathbf{H}_{\mathbf{d}-1}$  is the  $|\mathcal{L}_{d-1}| \times |\mathcal{L}_{d-1}|$  Hamiltonian along the remaining  $d-1$  directions and  $\tau_{\langle n+1,n \rangle}$  denotes the connectivity matrices along the transfer direction (cp. Fig. 2). The advantage of singling out a special direction along which to study wave function progression lies in the fact that 1D localization is mathematically known to be very strong which usually translates into fast algorithmic convergence.

With  $T_n$  the  $2|\mathcal{L}_{d-1}| \times 2|\mathcal{L}_{d-1}|$  (local transfer) matrix in (3), we define the global transfer matrix  $\mathcal{T}_{\mathcal{L}_{d-1}}(|\mathcal{L}_1|) = \prod_{n=1}^{|\mathcal{L}_1|} T_n$ . Then  $\lim_{|\mathcal{L}_1| \rightarrow \infty} (\mathcal{T}\mathcal{T}^\dagger) = \exp[2 \text{diag}(\gamma_1, \dots, \gamma_{2|\mathcal{L}_{d-1}|})|\mathcal{L}_1|]$  with Lyapunov decay exponents  $\gamma_1, \dots, \gamma_{2|\mathcal{L}_{d-1}|}$ , ordered  $\gamma_1 > \gamma_2 > \dots > \gamma_{|\mathcal{L}_{d-1}|} > 0 > -\gamma_{|\mathcal{L}_{d-1}|} > \dots > -\gamma_1$ , i.e. the Lyapunov exponents come in pairs  $\pm\gamma_m$ ,  $m = 1, \dots, |\mathcal{L}_{d-1}|$  due to the symplectic structure of the  $T_n$ . The positive  $\gamma_{\mathcal{L}_{d-1}}$  indicates the largest extend of the states along the transfer direction, leading to the definition of the (largest) localization length as  $\lambda_{\mathcal{L}_{d-1}} = 1/\gamma_{\mathcal{L}_{d-1}}$ . Implicit in the convergent construction of the  $\lambda_m = 1/\gamma_m$  is the self-averaging over the disorder along the transfer direction. An error analysis in the *statistical* changes in the  $\lambda_m$  has to be made when computing the stopping criterion of the TMM (MacKinnon and Kramer, 1983). The  $\mathcal{L}_{d-1}$  dependence of  $\lambda_{\mathcal{L}_{d-1}}$  lends itself to finite-size scaling and can hence be used to characterize universal properties of Anderson localization. A direct connection to the typical conductance is also known (Pichard and Sarma (1981)).

Generalizations of the TMM include different lattice structures (Schreiber and Ottomeier, 1992, Eilmes et al., 2008) as well as non-standard transfer directions (Frahm et al., 1995). For disorder distributions for whom self-averaging is not applicable, a forward/backward variant of the TMM has been given as well (Frahm et al., 1995, Ndawana et al., 2004). A recent reevaluation of the idea of self-averaging has also led to the first efficient implementation of TMM on massively-parallel computing architectures (Slevin and Ohtsuki, 2018).

Computing matrix elements of the resolvent  $(E\mathbf{1} - \mathbf{H}_{d-1})^{-1}$  leads to a conceptually very similar recursion setup compared to (3). This so-called Green function method (MacKinnon and Kramer, 1981) again provides access to localization lengths and conductivity for chosen values of  $\mathcal{L}_{d-1}$ . An implementation of the method along a non-standard transfer direction has been given by Von Oppen et al. (1996).

#### 4. Renormalization and decimation methods

Real-space renormalization approaches provide another starting point for studying Anderson localized systems. Here the idea is that an individual lattice site  $\mathbf{a}$  can be "removed" from  $\mathcal{L}$ , leading to a modified  $H_{\mathbf{a}\mathbf{b}}$ . For example, the decimation method (Aoki, 1982, Leadbeater et al., 1999), finds  $H'_{\mathbf{a},\mathbf{b}} = H_{\mathbf{a},\mathbf{b}} + (H_{\mathbf{a},|\mathcal{L}_d|}H_{|\mathcal{L}_d|,\mathbf{b}}) / (E - H_{|\mathcal{L}_d|,|\mathcal{L}_d|})$  after removal of the site  $|\mathcal{L}_d|$  while the Green function remains unchanged. In this way, the decimation of

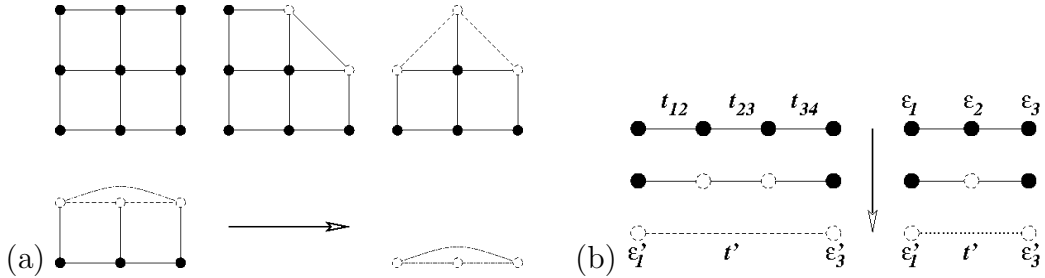


Figure 3: Schematic of real-space decimation procedures using (a) Green function renormalization in  $d = 2$  and (b) local energy renormalization for hopping (left of  $\downarrow$ ) and onsite terms (right of  $\downarrow$ ) in, e.g.,  $d = 1$ . In both schematics, solid lines and circles indicate unrenormalized hopping ( $t_{12}, t_{23}, t_{34}$ ) and onsite energies ( $\varepsilon_1, \varepsilon_2, \varepsilon_3$ ), respectively, while the dashed and dotted lines and circles represent renormalized values ( $t'$  and  $\varepsilon'_1, \varepsilon'_3$ ). The (a) horizontal and (b) vertical arrows represent to renormalization progression in both schemes.

lattice sites can proceed until a sufficiently small Hamiltonian has been constructed to use the exact diagonalization routines reviewed above (cp. Fig. 3(a)). Another recent variant of real-space normalization makes use of the information encoded in the  $\varepsilon_{\mathbf{a}}$  and  $t_{\mathbf{a},\mathbf{b}}$  values. By recursively elimination those sites with the largest local energy scale  $\Omega = \max_{\mathbf{a},\mathbf{b}} \{|\varepsilon_{\mathbf{a}}|, |t_{\mathbf{a},\mathbf{b}}|\}$ , (Javan Mard et al., 2014, Mard et al., 2017) continue until only a single renormalized link  $\varepsilon'_\alpha - t'_{\alpha,\beta} - \varepsilon'_\beta$  is left. This last link can then be used to compute transport properties, including their disorder  $W$  dependence and the scaling behaviour (cp. Fig. 3(b)). The method is applicable for  $1 \leq d < \infty$ . In  $d = 2$ , the approach is similar in spirit to the real-space renormalization approach used for localization in a magnetic field (Cain and Römer, 2005).

## 5. Energy-level statistics

The distribution of energy-level spacings  $\delta_n = E_{n+1} - E_n$  in the eigen-spectra  $\{E_n\}$  of Anderson-type systems has long been known to provide a marker able to distinguish between extended and localized eigenstates  $\Psi$  (Altshuler and Shklovskii, 1986, Evangelou and Economou, 1992, Shklovskii et al., 1993) with distribution functions  $P(\delta)$  of the spacing following the three Dyson ensembles — e.g. with the Gaussian orthogonal ensemble (GOE) corresponding to real-symmetric matrices invariant under orthogonal transformations — (Dyson, 1962, Shklovskii et al., 1993) and generalizations thereof (Altland and Zirnbauer, 1997). Often, the integrated distribution function

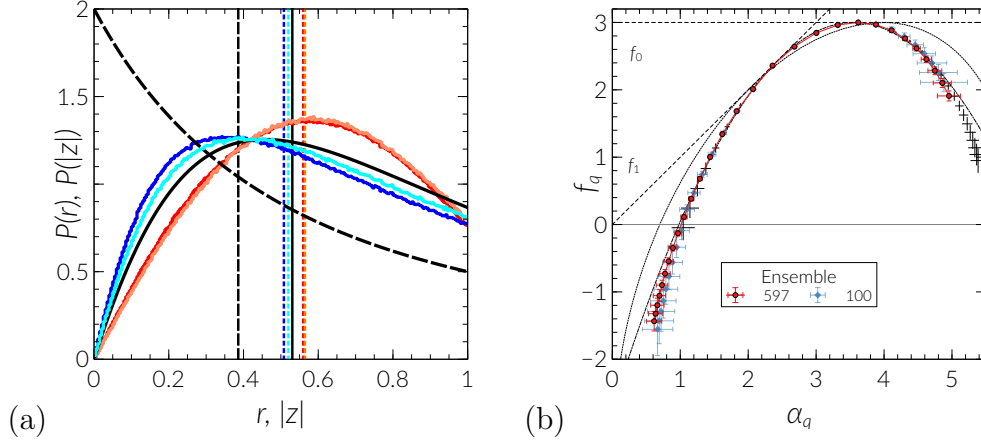


Figure 4: (a) Distributions of the energy level ratios  $r$  (dark and light blue) and  $|z|$  (dark and light red) for a  $d = 3$  Lieb model with  $44^3$  sites (Liu et al., 2020) and averaged over  $\sim 8 \times 10^6$  ratios for each curve. Darker colors denote slightly larger disorders. The black dashed and solid lines denote the exact  $P_{\text{Poisson}}(r)$  and a surmise for  $P_{\text{GOE}}(r)$ . No such predictions are yet known for  $P(|z|)$  (Luo et al., 2021). (b) Ensemble-averaged singularity spectrum  $f_q(\alpha_q)$ , parameterised by  $q$ -moments, for Kohn-Sham wave functions computed via density-functional theory of Si:P with  $22^3$  atoms of which 140 are P impurities (Carnio et al., 2019a). The spectrum has been sampled for values of  $q = 5, 4.75, \dots, -1.75, -2$  (decreasing from left to right) in the bulk of the impurity band at 0.2495 eV below the Fermi energy. Blue diamonds show the results for the ensemble of the first 100 disorder realisations, while red circles indicate the results from all 597 available realisations. Simple error bars, without data point, indicate the symmetrised spectrum of the full ensemble. Dashed lines indicate the functions  $f_0 \equiv 3$  and  $f_1(\alpha) = \alpha$ . The dotted line represents the spectrum for the standard cubic 3D Anderson model at criticality, reproduced from Rodriguez et al. (2011), while the dot-dashed line shows the fit to a parabolic approximation (Evers and Mirlin, 2008). The two horizontal lines are guides to  $f = 0$  and 3.



$I(\delta) = \int_0^\delta P(\delta') d\delta'$  is a numerically more stable indicator (Zhong et al., 1998). More detailed tests of the spectral properties such as the  $\Delta_3$  and  $\Sigma_2$  statistics have also been employed (Mehta, 2004, Hofstetter and Schreiber, 1993). As usual, the  $|\mathcal{L}_d|$  dependence of these quantities can be used for scaling; convenient estimates of  $P(s)$ , etc., have been given based on Wigner surmises (Shklovskii et al., 1993).

However, before a detailed comparison with predictions of random matrix theory is possible, the region of the spectrum under investigation has to be *unfolded* so that the unfolded density-of-states is constant Hofstetter and Schreiber (1993). This adds a possible source of numerical uncertainty for systems with large fluctuations in the density-of-states. Recently, it has been suggested to study ratios of level spacings such as  $0 \leq r_n = \min\{\delta_n, \delta_{n-1}\} / \max\{\delta_n, \delta_{n-1}\} \leq 1$  (Oganesyan and Huse, 2007) and others (Luo et al., 2021) and their distributions instead (cp. Fig. 4(a)). For such ratios, the unfolding procedure is no longer necessary, while mean and moments are still accessible via surmises and even exact results exist (Atas et al., 2013, Giraud et al., 2022).

## 6. Wavefunction statistics and multi-fractal analysis

Unsurprisingly, the properties of the eigenstates of (1) are also useful when studying the localization properties. In the simplest situation, the participation number  $\mathcal{P} = (\sum_{\mathbf{a} \in \mathcal{L}_d} |\Psi_{\mathbf{a}}|^4)^{-1}$  (Wegner, 1980) measures how many sites in  $\mathcal{L}_d$  *participate* in the spatial extend of a given  $\Psi$ . E.g. for a localized  $\Psi$ ,  $\mathcal{P} \sim 1$ , whereas for an extended  $\Psi$ ,  $\mathcal{P} \sim |\mathcal{L}_d|$ . The universal statistical properties of  $\Psi$  can be computed as well, with the Porter-Thomas distributions capturing the behaviour at weak disorder while the systematic corrections at larger disorder have been calculated in a series of works (Mirlin, 1999). Directly at the Anderson metal-insulator transition, e.g. in three-dimensions,  $\Psi$  has the scaling properties of a multifractal (Janssen, 1998). The full multifractal spectrum can be shown to be system-size independent and the moments of the multifractal distributions can be used to characterize the critical properties of the transition Rodriguez et al. (2011), via finite-size scaling. A typical multi-fractal  $f(\alpha)$  spectrum is shown in Fig. 4(b).

## 7. Finite-size scaling

The finite-size scaling approach to second order phase transitions has been well documented by now (Abrahams et al., 1979, Belitz and Kirkpatrick,

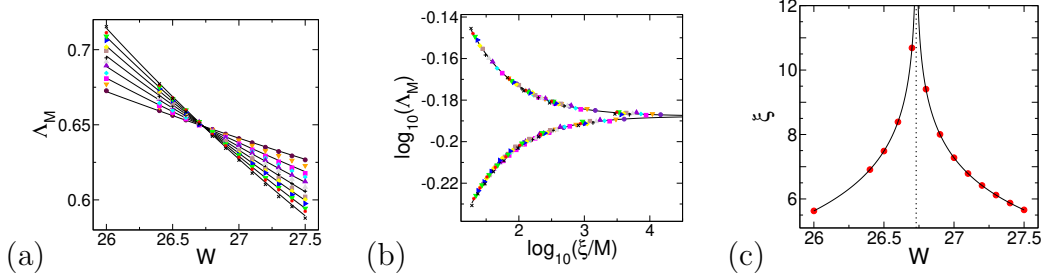


Figure 5: Reduced localization lengths  $\Lambda_M = \lambda_{|\mathcal{L}_2|}/M$ , with  $M = |\mathcal{L}_2|$  the size of the TMM bar, versus (a)  $W$  or (b)  $\xi(W)/M$  for  $E = 0$  of a  $d = 3$  Anderson model defined on an fcc lattice (Eilmes et al., 2008). Different symbols and colors denote increasing  $M = 3(\bullet), \dots, 15(\times)$ . Panel (c) shows the constructed  $\xi(W)$  scaling parameter function (black line) with divergence at  $W_c = 26.73(1)$  (vertical dotted line) and the computed  $\xi(W_i)$  values for  $W_i = 26, \dots, 27.5$  (circles).

1994, Slevin and Ohtsuki, 1999). Roughly speaking, finite-size scaling implies to collapse of data for different parameters such as  $E$  and  $W$  onto a single scaling curve when their system size  $|\mathcal{L}_d|$  dependence is adjusted as well (Slevin and Ohtsuki, 1999).

For the Anderson localization problem, there exist two different numerical approaches. In the absence of a phase transition, i.e. in  $d \leq 2$ , or when the functional form of the transition is not known, one can attempt to simply construct the data collapse of a suitably chosen quantity, such as the localization length  $\lambda_{|\mathcal{L}_d|}$  or a multifractal moment  $\tau_q$ , by minimization of the overlap between curves. In this approach, the shift needed to achieve this minimal overlap defines a scaling parameter  $\xi$  and its parameter dependence on  $E$  or  $W$ . For the Anderson transition in three dimensions, the behaviour should be a good approximation of  $\xi \propto |E - E_c|^{-\nu}$  or  $\xi \propto |W - W_c|^{-\nu}$ . This defines the critical transition points  $E_c$ ,  $W_c$  as well as the critical exponent  $\nu$ .

The second, more modern approach, starts by assuming a scaling form for  $\xi_{|\mathcal{L}_d|}$ , say

$$\xi_{|\mathcal{L}_d|}(F) = a_{00} + a_{01} (F/F_c - 1) |\mathcal{L}_d|^{1/\nu} + |\mathcal{L}_d|^{-y} \left[ a_{10} + a_{11} (F/F_c - 1) |\mathcal{L}_d|^{1/\nu} \right], \quad (4)$$

and then fits the parameters  $a_{ij}$ ,  $\nu$  and  $y$  to allow the best possible fit to the accumulated data points by a non-linear regression (Slevin and Ohtsuki, 1999) for either energy ( $F = E$ ) or disorder ( $F = W$ ) dependence (cp. Fig. 5). This more systematic approach allows the inclusion of the irrelevant

scaling exponent  $y > 0$  as shown in the example. The accuracy of a fit is quantified via  $\chi^2$  analysis. When constructing the scaling function  $\xi$  in powers of relevant and irrelevant corrections, one has to take care that the fit with the best  $\chi^2$  statistics is also robust with respect to changes in the considered range of energies and disorders considered as well as stable within the computed accuracy when increasing the complexity of the fit function. It is this second finite-size scaling approach, together with high accuracy data computed by the TMM or sparse matrix diagonalization coupled with multifractal analysis as outlined above which currently gives the accepted best-fit estimates of the critical properties at the Anderson transition (Slevin and Ohtsuki, 1999).

## 8. Localization and many-body interactions

The possibility of including the influence of interactions on the Anderson localization problem has always intrigued the community and was mentioned already by Anderson (1958). Numerically, the problem becomes much harder since the number of states in Hilbert space grows from  $\propto |\mathcal{L}_d|^d$  to  $\propto \exp |\mathcal{L}_d|$  while the requirement to perform the disorder averaging remains. Early investigations concentrated on studying the influence of disorder on the ground states of interacting systems. Mostly, progress was based on numerical methods adopted from clean interacting systems with methods such as the density-matrix renormalization group (White, 1992, Schollwöck, 2005) and exact diagonalization most commonly used. For the many-body localization problem (see Oganesyan article in this encyclopedia), the complete spectrum is often of much interest, so the exact diagonalization is often the method of choice, severely restricting the spatial size of systems while still retaining a relatively large Hilbert space (Oganesyan and Huse, 2007). Alternative renormalization schemes such as implementations of the strong-disorder renormalization group (Hikihara et al., 1999, Goldsborough and Römer, 2014), already mentioned above for the non-interacting case, might also provide a way forward.

More recently, approximate methods such as the time-honoured Hartree-Fock (Weidinger et al., 2018, Oswald and Römer, 2020) as well as density-functional-theory methods (Harashima and Slevin, 2014, Carnio et al., 2019b) have begun to be applied. Particularly the latter offer the exciting possibility of providing a material-specific approach to studies of Anderson localization (Carnio et al., 2019a). In this context, one should also mention the typical medium dynamical cluster approximation for disordered electronic systems

(Aguiar et al., 2009) which can now also be used to incorporate density-functional-theory-derived potentials, the effect of multiple bands, non-local disorder, and electron-electron interactions (Terletska et al., 2018). Another approximate method that incorporates the full spatial variations of wave functions and *local* interactions effects is the Statistical Dynamical Mean Field Theory (Dobrosavljević and Kotliar, 1997, Miranda and Dobrosavljević, 2012). Local interactions are included self-consistently through effective correlated single-impurity problems (CSIP) (Georges et al., 1996). In the disordered context, each site defines a different CSIP whose local self-energy is fed back into the lattice self-consistent loop. In the non-interacting limit the formulation is exact. It has been used to study the disordered Mott transition (Miranda and Dobrosavljević, 2012, Suárez-Villagrán et al., 2020) and disordered heavy fermion systems (Miranda and Dobrosavljević, 2001), where a distribution of Kondo temperatures is a conceptually useful byproduct.

## 9. Machine learning

A seemingly new approach has become available to the numerical study of Anderson localization with the emergence of the machine learning paradigm. Instead of specifying in detail which physical aspects of data to concentrate on, say transport properties such as  $\lambda$ , conductivity or multifractal moments  $\tau_q$ , the data-driven machine learning approach can be used to find Anderson transitions for variants of the model Hamiltonian (1) when training deep learning networks on, e.g., the standard cubic Anderson model Ohtsuki and Ohtsuki (2016). With this form of *supervised* machine learning of Anderson localization, Ohtsuki and Mano (2020) found that one can determine phase diagrams in other disordered systems such as topological insulators and disordered Weyl semimetals (see the entries by ??? in the encyclopedia). How other machine learning strategies such as unsupervised and reinforcement learning might add to the numerical approaches for Anderson localization is currently under much investigation.

## 10. Conclusions

In this entry to the encyclopedia, I have attempted to provide a very brief review of the rich variety of numerical algorithms developed to study Anderson localization. Due to brevity requirements appropriate for such

an entry, details had to be mostly neglected. Still, with citations provided to hopefully the original publications as well as some recent examples, I hope that the reader can find enough information to get started with each approach and that seeing them in context allows for a considered choice of which method to use.

### *Acknowledgments*

I am grateful for constructive suggestions on the manuscript by H. Fehske, E. Miranda, A. Rodriguez and T. Ohtsuki. Special thanks to E. Carnio for help with Fig. 4.

### **References**

- E. Abrahams, P. W. Anderson, D. C. Licciardello, and T. V. Ramakrishnan. Scaling Theory of Localization: Absence of Quantum Diffusion in Two Dimensions. *Physical Review Letters*, 42(10):673–676, 3 1979. ISSN 0031-9007. doi: 10.1103/PhysRevLett.42.673. URL <https://link.aps.org/doi/10.1103/PhysRevLett.42.673>.
- M. C. O. Aguiar, V. Dobrosavljević, E. Abrahams, and G. Kotliar. Critical behavior at the Mott-Anderson transition: A typical-medium theory perspective. *Physical Review Letters*, 102(15), 2009. ISSN 00319007. doi: 10.1103/PhysRevLett.102.156402. URL <http://link.aps.org/doi/10.1103/PhysRevLett.102.156402>.
- A. Altland and M. R. Zirnbauer. Nonstandard symmetry classes in mesoscopic normal-superconducting hybrid structures. *Physical Review B*, 55(2):1142, 1 1997. ISSN 1550235X. doi: 10.1103/PhysRevB.55.1142. URL <https://journals.aps.org/prb/abstract/10.1103/PhysRevB.55.1142>.
- B. L. Altshuler and B. I. Shklovskii. Repulsion of energy levels and conductivity of small metal samples. *Zhurnal Eksperimentalnoi I Teoreticheskoi Fiziki*, 91(July 1986):220–234, 1986.
- E. Anderson, Z. Bai, C. Bischof, L. S. Blackford, J. Demmel, J. Dongarra, J. Du Croz, A. Greenbaum, S. Hammarling, A. McKenney, and D. Sorensen. *LAPACK Users' Guide*. Society for Industrial and Applied Mathematics, 1 1999. ISBN 978-0-89871-447-0. doi: 10.1137/

- 1.9780898719604. URL <http://epubs.siam.org/doi/book/10.1137/1.9780898719604>.
- P. W. Anderson. Absence of Diffusion in Certain Random Lattices. *Physical Review*, 109(5):1492–1505, 3 1958. ISSN 0031-899X. doi: 10.1103/PhysRev.109.1492. URL <https://link.aps.org/doi/10.1103/PhysRev.109.1492>.
- H. Aoki. Decimation method of real-space renormalization for electron systems with application to random systems. *Physica A: Statistical Mechanics and its Applications*, 114(1-3):538–542, 8 1982. ISSN 03784371. doi: 10.1016/0378-4371(82)90345-4. URL <https://linkinghub.elsevier.com/retrieve/pii/0378437182903454>.
- Y. Y. Atas, E. Bogomolny, O. Giraud, P. Vivo, and E. Vivo. Joint probability densities of level spacing ratios in random matrices. *Journal of Physics A: Mathematical and Theoretical*, 46(35):355204, 9 2013. ISSN 1751-8113. doi: 10.1088/1751-8113/46/35/355204. URL <https://iopscience.iop.org/article/10.1088/1751-8113/46/35/355204>.
- D. Belitz and T. R. Kirkpatrick. The Anderson-Mott transition. *Reviews of Modern Physics*, 66(2):261–380, 4 1994. ISSN 0034-6861. doi: 10.1103/RevModPhys.66.261. URL <https://link.aps.org/doi/10.1103/RevModPhys.66.261>.
- M. Bollhöfer and Y. Notay. JADAMILU: a software code for computing selected eigenvalues of large sparse symmetric matrices. *Computer Physics Communications*, 177(12):951–964, 2007. ISSN 00104655. doi: 10.1016/j.cpc.2007.08.004.
- T. Brandes and S. Kettemann. *Anderson Localization and Its Ramifications*, volume 630 of *Lecture Notes in Physics*. Springer Berlin Heidelberg, Berlin, Heidelberg, 2003. ISBN 978-3-540-40785-0. doi: 10.1007/b13139. URL <http://link.springer.com/10.1007/b13139>.
- P. Cain and R. A. Römer. Real-space renormalization-group approach to the integer quantum Hall effect. *International Journal of Modern Physics B*, 19(13):2085–2119, 5 2005. ISSN 0217-9792. doi: 10.1142/S0217979205029742. URL <https://www.worldscientific.com/doi/abs/10.1142/S0217979205029742>.

- E. G. Carnio, N. D. Hine, and R. A. Römer. Multifractality of ab initio wave functions in doped semiconductors. *Physica E: Low-dimensional Systems and Nanostructures*, 111:141–147, 7 2019a. ISSN 13869477. doi: 10.1016/j.physe.2019.02.020. URL <https://linkinghub.elsevier.com/retrieve/pii/S1386947719300104>.
- E. G. Carnio, N. D. M. Hine, and R. A. Römer. Resolution of the exponent puzzle for the Anderson transition in doped semiconductors. *Physical Review B*, 99(8):081201(R), 2 2019b. ISSN 2469-9950. doi: 10.1103/PhysRevB.99.081201. URL <http://arxiv.org/abs/1710.01742><https://link.aps.org/doi/10.1103/PhysRevB.99.081201>.
- J. K. Cullum and R. A. Willoughby. *Lanczos Algorithms for Large Symmetric Eigenvalue Computations*. Society for Industrial and Applied Mathematics, 1 2002. ISBN 978-0-89871-523-1. doi: 10.1137/1.9780898719192. URL <http://epubs.siam.org/doi/book/10.1137/1.9780898719192>.
- V. Dobrosavljević and G. Kotliar. Mean Field Theory of the Mott-Anderson Transition. *Physical Review Letters*, 78(20):3943–3946, 5 1997. ISSN 0031-9007. doi: 10.1103/PhysRevLett.78.3943. URL <https://link.aps.org/doi/10.1103/PhysRevLett.78.3943>.
- F. J. Dyson. Statistical Theory of the Energy Levels of Complex Systems. I. *Journal of Mathematical Physics*, 3(1):140–156, 1 1962. ISSN 0022-2488. doi: 10.1063/1.1703773. URL <http://aip.scitation.org/doi/10.1063/1.1703773>.
- A. Eilmes, A. M. Fischer, and R. A. Römer. Critical parameters for the disorder-induced metal-insulator transition in fcc and bcc lattices. *Physical Review B*, 77(24):245117, 6 2008. ISSN 1098-0121. doi: 10.1103/PhysRevB.77.245117. URL <https://link.aps.org/doi/10.1103/PhysRevB.77.245117>.
- S. N. Evangelou and E. N. Economou. Spectral density singularities, level statistics, and localization in a sparse random matrix ensemble. *Physical Review Letters*, 68(3):361, 1 1992. ISSN 00319007. doi: 10.1103/PhysRevLett.68.361. URL <https://journals.aps.org/prl/abstract/10.1103/PhysRevLett.68.361>.

- F. Evers and A. D. Mirlin. Anderson transitions. *Reviews of Modern Physics*, 80(4):1355–1417, 2008. ISSN 00346861. doi: 10.1103/RevModPhys.80.1355. URL <http://link.aps.org/doi/10.1103/RevModPhys.80.1355>.
- K. Frahm, A. Müller-Groeling, J.-L. Pichard, and D. Weinmann. Scaling in Interaction-Assisted Coherent Transport. *Europhysics Letters (EPL)*, 31(3):169–174, 7 1995. ISSN 0295-5075. doi: 10.1209/0295-5075/31/3/008. URL <https://iopscience.iop.org/article/10.1209/0295-5075/31/3/008>.
- A. Georges, G. Kotliar, W. Krauth, and M. J. Rozenberg. Dynamical mean-field theory of strongly correlated fermion systems and the limit of infinite dimensions. *Reviews of Modern Physics*, 68(1):13–125, 1 1996. ISSN 0034-6861. doi: 10.1103/RevModPhys.68.13. URL <https://link.aps.org/doi/10.1103/RevModPhys.68.13>.
- O. Giraud, N. Macé, E. Vernier, and F. Alet. Probing Symmetries of Quantum Many-Body Systems through Gap Ratio Statistics. *Physical Review X*, 12(1):011006, 3 2022. ISSN 21603308. doi: 10.1103/PhysRevX.12.011006/FIGURES/9/MEDIUM. URL <https://journals.aps.org/prx/abstract/10.1103/PhysRevX.12.011006>.
- A. M. Goldsborough and R. A. Römer. Self-assembling tensor networks and holography in disordered spin chains. *Physical Review B*, 89(21):214203, 6 2014. ISSN 1098-0121. doi: 10.1103/PhysRevB.89.214203. URL <https://link.aps.org/doi/10.1103/PhysRevB.89.214203>.
- Y. Harashima and K. Slevin. Critical exponent of metal-insulator transition in doped semiconductors: The relevance of the Coulomb interaction. *Physical Review B*, 89:205108, 2014. ISSN 1098-0121. doi: 10.1103/PhysRevB.89.205108. URL <http://link.aps.org/doi/10.1103/PhysRevB.89.205108>.
- T. Hikihara, A. Furusaki, and M. Sgrist. Numerical renormalization-group study of spin correlations in one-dimensional random spin chains. *Physical Review B*, 60(17):12116–12124, 11 1999. ISSN 0163-1829. doi: 10.1103/PhysRevB.60.12116. URL <https://link.aps.org/doi/10.1103/PhysRevB.60.12116>.



- E. Hofstetter and M. Schreiber. Statistical properties of the eigenvalue spectrum of the three-dimensional Anderson Hamiltonian. *Physical Review B*, 48(23):16979, 12 1993. ISSN 01631829. doi: 10.1103/PhysRevB.48.16979. URL <https://0-journals-aps-org.pugwash.lib.warwick.ac.uk/prb/abstract/10.1103/PhysRevB.48.16979>.
- R. A. Horn and C. R. Johnson. Matrix Analysis(2nd Edtion). *Cambridge University Press*, 1985. URL <https://www.cambridge.org/core/product/identifier/9780511810817/type/book>.
- M. Janssen. Statistics and scaling in disordered mesoscopic electron systems. *Physics Reports*, 295(1-2):1–91, 3 1998. ISSN 03701573. doi: 10.1016/S0370-1573(97)00050-1. URL <https://linkinghub.elsevier.com/retrieve/pii/S0370157397000501>.
- H. Javan Mard, J. A. Hoyos, E. Miranda, and V. Dobrosavljević. Strong-disorder renormalization-group study of the one-dimensional tight-binding model. *Physical Review B*, 90(12):125141, 9 2014. ISSN 1098-0121. doi: 10.1103/PhysRevB.90.125141. URL <https://link.aps.org/doi/10.1103/PhysRevB.90.125141>.
- B. Kramer and A. MacKinnon. Localization: theory and experiment. *Reports on Progress in Physics*, 56(12):1469–1564, 12 1993. ISSN 0034-4885. doi: 10.1088/0034-4885/56/12/001. URL <https://iopscience.iop.org/article/10.1088/0034-4885/56/12/001>.
- M. Leadbeater, R. Römer, and M. Schreiber. Interaction-dependent enhancement of the localisation length for two interacting particles in a one-dimensional random potential. *The European Physical Journal B*, 8(4): 643–652, 4 1999. ISSN 1434-6028. doi: 10.1007/s100510050732. URL <http://link.springer.com/10.1007/s100510050732>.
- J. Liu, X. Mao, J. Zhong, and R. A. Römer. Localization, phases, and transitions in three-dimensional extended Lieb lattices. *Physical Review B*, 102(17):174207, 11 2020. ISSN 2469-9950. doi: 10.1103/PhysRevB.102.174207. URL <https://link.aps.org/doi/10.1103/PhysRevB.102.174207>.
- X. Luo, T. Ohtsuki, and R. Shindou. Universality Classes of the Anderson Transitions Driven by Non-Hermitian Disorder. *Physical Review Let-*

- ters*, 126(9):90402, 2021. ISSN 10797114. doi: 10.1103/PhysRevLett.126.090402. URL <https://doi.org/10.1103/PhysRevLett.126.090402>.
- A. MacKinnon and B. Kramer. One-Parameter Scaling of Localization Length and Conductance in Disordered Systems. *Physical Review Letters*, 47(21):1546, 11 1981. ISSN 00319007. doi: 10.1103/PhysRevLett.47.1546. URL <https://0-journals-aps-org.pugwash.lib.warwick.ac.uk/prl/abstract/10.1103/PhysRevLett.47.1546>.
- A. MacKinnon and B. Kramer. The scaling theory of electrons in disordered solids: Additional numerical results. *Zeitschrift für Physik B Condensed Matter*, 53(1):1–13, 3 1983. ISSN 0722-3277. doi: 10.1007/BF01578242. URL <http://link.springer.com/10.1007/BF01578242>.
- H. J. Mard, J. A. Hoyos, E. Miranda, and V. Dobrosavljević. Strong-disorder approach for the Anderson localization transition. *Physical Review B*, 96(4):045143, 7 2017. ISSN 2469-9950. doi: 10.1103/PhysRevB.96.045143. URL <http://arxiv.org/abs/1412.3793><http://link.aps.org/doi/10.1103/PhysRevB.96.045143>.
- M. L. Mehta. Random Matrices. *Academic Press*, page 706, 2004. URL [http://store.elsevier.com/product.jsp?isbn=9780120884094&\\_requestid=513396](http://store.elsevier.com/product.jsp?isbn=9780120884094&_requestid=513396).
- E. Miranda and V. Dobrosavljevic. Localization-Induced Griffiths Phase of Disordered Anderson Lattices. *Physical Review Letters*, 86(2):264, 1 2001. ISSN 00319007. doi: 10.1103/PhysRevLett.86.264. URL <https://journals.aps.org/prl/abstract/10.1103/PhysRevLett.86.264>.
- E. Miranda and V. Dobrosavljević. Dynamical Mean-field Theories of Correlation and Disorder. In V. Dobrosavljević, N. Trivedi, and J. M. Valles, editors, *Conductor-Insulator Quantum Phase Transitions*, volume 9780199592, pages 161–243. Oxford University Press, Oxford, UK, 1st edition, 6 2012. ISBN 9780191741050. doi: 10.1093/acprof:oso/9780199592593.003.0006. URL <https://oxford.universitypressscholarship.com/view/10.1093/acprof:oso/9780199592593.001.0001/acprof-9780199592593-chapter-6>.
- A. D. Mirlin. Correlations of Wave Functions in Disordered Systems. In I. Lerner, J. Keating, and D. Khmelnitskii, editors, *Supersymmetry and*

- Trace Formulae*, pages 245–260. Springer, Boston, MA, Boston, MA, nato asi s edition, 1999. doi: 10.1007/978-1-4615-4875-1{\\_}12. URL [http://link.springer.com/10.1007/978-1-4615-4875-1\\_12](http://link.springer.com/10.1007/978-1-4615-4875-1_12).
- M. L. Ndwana, R. A. Römer, and M. Schreiber. The Anderson metal-insulator transition in the presence of scale-free disorder. *Europhysics Letters (EPL)*, 68(5):678–684, 12 2004. ISSN 0295-5075. doi: 10.1209/epl/i2004-10267-5. URL <https://iopscience.iop.org/article/10.1209/epl/i2004-10267-5>.
- V. Oganessian and D. A. Huse. Localization of interacting fermions at high temperature. *Physical Review B*, 75(15):155111, 4 2007. ISSN 1098-0121. doi: 10.1103/PhysRevB.75.155111. URL <https://link.aps.org/doi/10.1103/PhysRevB.75.155111>.
- T. Ohtsuki and T. Mano. Drawing Phase Diagrams of Random Quantum Systems by Deep Learning the Wave Functions. *Journal of the Physical Society of Japan*, 89(2):022001, 2 2020. ISSN 0031-9015. doi: 10.7566/JPSJ.89.022001. URL <https://arxiv.org/abs/1909.09821><http://dx.doi.org/10.7566/JPSJ.89.022001>.
- T. Ohtsuki and T. Ohtsuki. Deep learning the quantum phase transitions in random two-dimensional electron systems. *Journal of the Physical Society of Japan*, 85(12), 2016. ISSN 13474073. doi: 10.7566/JPSJ.85.123706. URL <http://journals.jps.jp/doi/pdf/10.7566/JPSJ.85.123706>.
- J. Oswald and R. A. Römer. Microscopic details of stripes and bubbles in the quantum Hall regime. *Physical Review B*, 102(12):121305, 9 2020. ISSN 2469-9950. doi: 10.1103/PhysRevB.102.121305. URL <http://arxiv.org/abs/2001.07542><https://link.aps.org/doi/10.1103/PhysRevB.102.121305>.
- J. L. Pichard and G. Sarma. Finite size scaling approach to Anderson localisation. *Journal of Physics C: Solid State Physics*, 14(6), 1981. ISSN 00223719. doi: 10.1088/0022-3719/14/6/003.
- A. Rodriguez, L. J. Vasquez, K. Slevin, and R. A. Römer. Multifractal finite-size scaling and universality at the Anderson transition. *Physical Review B*, 84(13):134209, 10 2011. ISSN 1098-0121. doi: 10.1103/PhysRevB.

- 84.134209. URL <https://link.aps.org/doi/10.1103/PhysRevB.84.134209>.
- O. Schenk, M. Bollhöfer, and R. A. Römer. On Large-Scale Diagonalization Techniques for the Anderson Model of Localization. *SIAM Review*, 50(1): 91–112, 1 2008. ISSN 0036-1445. doi: 10.1137/070707002. URL <http://epubs.siam.org/doi/10.1137/070707002>.
- U. Schollwöck. The density-matrix renormalization group. *Reviews of Modern Physics*, 77(1):259–315, 2005. ISSN 0034-6861. doi: 10.1103/RevModPhys.77.259. URL <https://link.aps.org/doi/10.1103/RevModPhys.77.259>.
- M. Schreiber and M. Ottomeier. Localization of electronic states in 2D disordered systems. *Journal of Physics: Condensed Matter*, 4(8):1959–1971, 2 1992. ISSN 0953-8984. doi: 10.1088/0953-8984/4/8/011. URL <https://iopscience.iop.org/article/10.1088/0953-8984/4/8/011>.
- B. I. Shklovskii, B. Shapiro, B. R. Sears, P. Lambrianides, and H. B. Shore. Statistics of spectra of disordered systems near the metal-insulator transition. *Physical Review B*, 47(17):11487, 5 1993. ISSN 01631829. doi: 10.1103/PhysRevB.47.11487. URL <https://0-journals-aps-org.pugwash.lib.warwick.ac.uk/prb/abstract/10.1103/PhysRevB.47.11487>.
- K. Slevin and T. Ohtsuki. Corrections to Scaling at the Anderson Transition. *Physical Review Letters*, 82(2):382–385, 1999. URL <http://link.aps.org/doi/10.1103/PhysRevLett.82.382>.
- K. Slevin and T. Ohtsuki. Critical Exponent of the Anderson Transition Using Massively Parallel Supercomputing. *Journal of the Physical Society of Japan*, 87(9):094703, 9 2018. ISSN 0031-9015. doi: 10.7566/JPSJ.87.094703. URL <http://arxiv.org/abs/1805.11781><http://dx.doi.org/10.7566/JPSJ.87.094703><https://journals.jps.jp/doi/10.7566/JPSJ.87.094703>.
- P. Stollmann. *Caught by Disorder*. Birkhäuser Boston, Boston, MA, 2001. ISBN 978-1-4612-6644-0. doi: 10.1007/978-1-4612-0169-4. URL <http://link.springer.com/10.1007/978-1-4612-0169-4>.

- M. Y. Suárez-Villagrán, N. Mitsakos, T. H. Lee, V. Dobrosavljević, J. H. Miller, and E. Miranda. Two-dimensional disordered Mott metal-insulator transition. *Physical Review B*, 101(23):235112, 6 2020. ISSN 24699969. doi: 10.1103/PHYSREVB.101.235112/FIGURES/14/MEDIUM. URL <https://journals.aps.org/prb/abstract/10.1103/PhysRevB.101.235112>.
- H. Terletska, Y. Zhang, K.-M. Tam, T. Berlijn, L. Chioncel, N. Vidhyadhiraja, and M. Jarrell. Systematic Quantum Cluster Typical Medium Method for the Study of Localization in Strongly Disordered Electronic Systems. *Applied Sciences*, 8(12):2401, 11 2018. ISSN 2076-3417. doi: 10.3390/app8122401. URL <http://arxiv.org/abs/1810.04728><http://www.mdpi.com/2076-3417/8/12/2401>.
- F. Von Oppen, T. Wettig, and J. Müller. Interaction-Induced Delocalization of Two Particles in a Random Potential: Scaling Properties. *Physical Review Letters*, 76(3):491, 1 1996. ISSN 10797114. doi: 10.1103/PhysRevLett.76.491. URL <https://journals.aps.org/prl/abstract/10.1103/PhysRevLett.76.491>.
- F. Wegner. Inverse participation ratio in  $2+?$  dimensions. *Zeitschrift für Physik B Condensed Matter and Quanta*, 36(3):209–214, 9 1980. ISSN 0340-224X. doi: 10.1007/BF01325284. URL <http://link.springer.com/10.1007/BF01325284>.
- S. A. Weidinger, S. Gopalakrishnan, and M. Knap. Self-consistent Hartree-Fock approach to many-body localization. *Physical Review B*, 98(22):224205, 12 2018. ISSN 24699969. doi: 10.1103/PHYSREVB.98.224205/FIGURES/11/MEDIUM. URL <https://journals.aps.org/prb/abstract/10.1103/PhysRevB.98.224205>.
- A. Weiße, G. Wellein, A. Alvermann, and H. Fehske. The kernel polynomial method. *Reviews of Modern Physics*, 78(1):275–306, 3 2006. ISSN 0034-6861. doi: 10.1103/RevModPhys.78.275. URL <https://link.aps.org/doi/10.1103/RevModPhys.78.275>.
- S. R. White. Density matrix formulation for quantum renormalization groups. *Physical Review Letters*, 69(19):2863, 11 1992. ISSN 00319007. doi: 10.1103/PhysRevLett.69.2863. URL <https://0-journals-aps-org.pugwash.lib.warwick.ac.uk/prl/abstract/10.1103/PhysRevLett.69.2863>.

J. X. Zhong, U. Grimm, R. A. Römer, and M. Schreiber. Level-Spacing Distributions of Planar Quasiperiodic Tight-Binding Models. *Physical Review Letters*, 80(18):3996–3999, 5 1998. ISSN 0031-9007. doi: 10.1103/PhysRevLett.80.3996. URL <http://arxiv.org/abs/cond-mat/9710006><https://link.aps.org/doi/10.1103/PhysRevLett.80.3996>.